Journal of Environment and Earth Science
ISSN 2224-3216 (Paper) ISSN 2225-0948 (Online)
Vol.5, No.6, 2015

Rippability Potential of the Near Surface Deposits of Jubilee Homes Parkland, Southwest, Nigeria

Rotimi O. J.* Atunbi J. F. Enaworu E. Ameloko A. A.
Petroleum Engineering Department, Covenant University, Ota, Nigeria
*E-mail of corresponding author: oluwatosin.rotimi@covenantuniversity.edu.ng; tossynrotimmy@yahoo.com

Abstract
Seismic refraction method of geophysical investigation has being used over the years in investigating subsurface formations and most importantly in identifying depth to bedrock. This has found application in both engineering and geoscience disciplines. Ripping or removal of rock beds for construction purposes may be due to urbanization or industrialization which is basically an environmentally influenced approach to optimizing operation, safety and durability. This study analyzed the rippability potential of sedimentary rocks of a parkland in Southwest Nigeria. Seismic refraction survey was employed to realize velocity of various lithology units the generated shock waves traversed and based on this, the rippability potential was inferred. Most profile location has three layers delineated while a fourth layer was delineated in some few locations. Average velocity for layers are 740 m/s, 1535.21 m/s, 2310 m/s and 2900 m/s for layers 1, 2, 3 and 4 respectively. The maximum vertical thickness is in excess of 12 m. The rock units are highly-weathered to weathered, therefore rippability is between easy and hard and achievable.
Keywords: Seismic; refraction; rippability; density; sedimentary rocks; construction; groundwater

1. Introduction

Rock uniaxial strength, degree or extent of weathering, structural properties and abrasiveness are numerous indices upon which rippability of rocks are based (Bienawski, 1973; Bailey, 1975; Smith, 1986; Earthworks, 2003). Sedimentary rocks are known to be most rippable. This is partly because they often exist without planes of weaknesses like cleavage or schistocity. However, their stratification or lamination patterns may constitute positively to their rippability. According to Smith (1986), physical characteristics such as frequent planes of weakness, weathering, moisture content, stratification, brittleness, low shear strength and low seismic velocities are favourable for ripping. Whereas, massive unlayered crystalline rocks with high shear strength and high seismic velocity are often difficult to rip (Caterpillar, 2010).

Over the years, refraction seismic has been used successfully in deducing rock velocities for purposes ranging from environmental, engineering to geological and others. This study makes an assessment of a virgin location that is opening up to urbanization and construction of industrial and residential facilities for the subsurface rocks rippability potentials towards siting structures. Erection of structures and making basic amenities available are the primary pointers to urbanization. The ground water potential of this area has been studied and documented in Rotimi *et al.,* 2014, and this serves as a report of further subsurface geophysical soundings carried out in the study area. Bedrocks are believed to be denser than regolith and top soil variants, they are expected to be competent and most resistant to weathering and movement and thus carry the weight of constructions such as building and road without failure. Hence, seismic refraction method of geophysical investigation is arguably the best and most field efficient method for determining the velocity to bedrock (Church, 1974). The increase of velocity with depth is the natural concept upon which seismic refraction thrives, however if the inverse becomes the case then there is a cause for concern.

1.1 Theory of Seismic Refraction

Understanding the theories in seismic refraction is based on the awareness that the subsurface is composed of a series of layers separated by plane and even dipping interfaces. Seismic velocities are also uniform within each layer and layer velocities increase with depth such that raypaths are restricted to vertical plane containing the profile line.

1.1.1 Two Layer Case

Suppose we have a case of flat interface between two horizontal layers as illustrated in Figure 1.

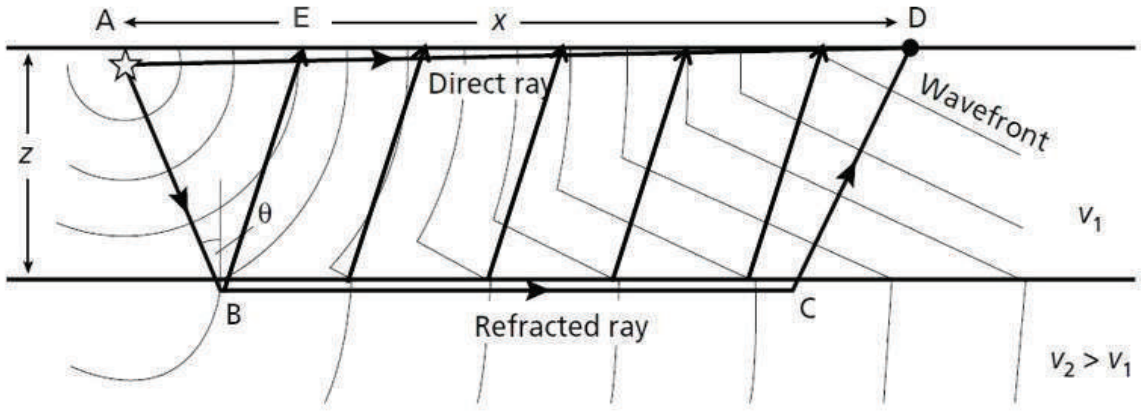

Figure 1: Direct, reflected and refracted wave along the horizontal interface between 2 layers.

From Figure 1, A indicates the source from where shock energy is released, B and C are points of detection of reflected ray and the distance between source S and detector D is X. Equations 1 to 26 represents a stepwise approach to computing depth to bedrock in seismic refraction. The velocity in medium 1 or first layer is V_1 and that of medium 2 or second layer is V_2 (assuming that $V_2 > V_1$). Then travel time t is $^X/_{V1}$ which gives us the distance-time curve for the direct wave as shown in Figure 2 where straight line passes through the origin to give a slope G which is equal to the inverse of the velocity, hence $G_1 = {}^1/_{V1}$ (Reynolds, 1997; Sharma, 1997; Kearey *et al.,* 2002). The refracted ray then travels to the interface B and then follows the path BC on the surface of a deeper layer where a velocity V_2 operates, the ray then bounces back to the surface along the path CD which is inclined at the critical angle $\boldsymbol{\theta}$.

It then follows that the travel time along refracted raypath ABCD is

$$t = t_{AB} + t_{BC} + t_{CD} \quad (1)$$

But $$t_{AB} = \frac{AB}{V_1} \quad (2)$$

Where $$AB = \frac{Z}{cos\theta} \quad (3)$$

Therefore,

$$t_{AB} = \frac{Z}{Vcos\theta} \quad (4)$$

On the other hand

$$t_{BC} = \frac{BC}{V_2} \quad (5)$$

But $$AB = AD - 2(BE) = X - 2(BE) \quad (6)$$

Where

$$BE = tan\theta \quad (7)$$

Therefore,

$$BC = X - 2Ztan\theta \quad (8)$$

Then;

$$t_{BC} = \frac{X-2Ztan\theta}{V_2} \quad (9)$$

$$t_{CD} = t_{AB} \quad (10)$$

$$t_{CD} = \frac{Z}{V_1 cos\theta} \quad (11)$$

Substituting equations 4, 9 and 11 into 1, gives equation 12 below

$$t = \frac{Z}{V_1 cos\theta} - \frac{X-2Ztan\theta}{V_2} + \frac{Z}{V_1 cos\theta} \quad (12)$$

$$= \frac{2Z}{V_1 cos\theta} + \frac{X-2Ztan\theta}{V_2 cos\theta} \quad (13)$$

$$= \frac{X}{V_2} + \frac{2Z}{V_1 cos\theta}\left\{\frac{1-V_1 sin\theta}{V_2}\right\} \quad (14)$$

$$= \frac{X}{V_2} + \frac{2Z\cos\theta}{V_1} \quad (15)$$

Since

$$\sin\theta = \frac{V_1}{V_2} \quad (16)$$

Equation (15) can be take the form in equation 17

$$t = \frac{2Z\cos\theta}{V_1} + \frac{X\sin\theta}{V_1} \quad (17)$$

Since

$$\cos\theta = \left\{1 - \left(\frac{V_1}{V_2}\right)^2\right\}^{1/2} \quad (18)$$

Then it becomes

$$t = \frac{X}{V_2} + 2Z\frac{(V_2 - V_1)^{1/2}}{V_1 V_2} \quad (19)$$

Plotting a time distance curve a slope of $G_2 = {}^1/_{V2}$ will be derived and the intercept of the curve t_1, where t_1=intercept time

Hence, it can be given as

$$t = 2Z\frac{(V_2^2 - V_1^2)^{1/2}}{V_1 V_2} \quad (20)$$

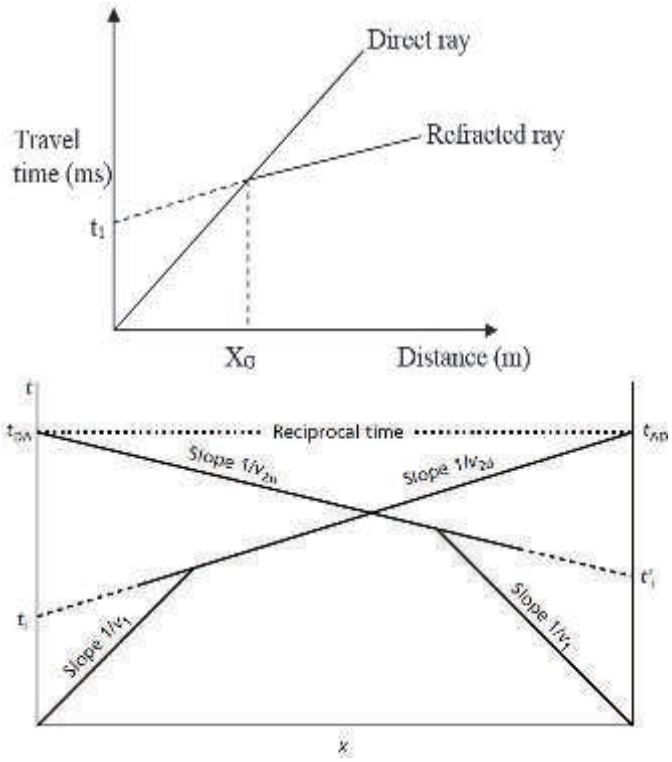

Figure 2: Time-Distance Curves. Left is for forward shooting. Right is for forward and reverse shooting.

Close to the shot point, the direct ray is the first to be recorded. The faster velocity of the lower layer is the refracted ray and this overtakes the direct ray to obtain the first arrival. The point where the refracted and the direct ray meet is called the *crossover point*, then when traced to the horizontal axis we obtain the *crossover distance*X_{cr} (Kearey *et al.,* 2002). In order to compute X_{cr}, the travel times for the direct and the refracted rays are equated as:

$$\frac{X}{V_1} = \frac{X}{V_2} + 2Z\frac{(V_2^2 - V_1^2)^{1/2}}{V_1 V_2} \quad (21)$$

Similarly

$$\frac{X_{cr}}{V_1} = \frac{X_{cr}}{V_2} + 2Z\frac{(V_2^2 - V_1^2)^{1/2}}{V_1 V_2} \quad (22)$$

$$X_{cr} = 2Z\frac{(v_2^2+v_1^2)^{1/2}}{(v_1-v_2)} \quad (23)$$

By implication therefore equation (23) shows that X_{cr} is more than twice the depth to the refractor.

1.1.2 Depth Calculation

To calculate the depth Z from the time-distance curve (Figure 2), the intercept time t_1 needs to be considered, hence using equation (21)

$$Z = \frac{t_1 v_2 v_1}{2(v_2^2-v_1^2)^{1/2}} \quad (24)$$

OR

$$Z = \frac{X_{cr}(v_2-v_1)^{1/2}}{2(v_2+v_1)} \quad (25)$$

Since

$$t_1 = t - \frac{X}{v_2} \quad (26)$$

1.2 Concept of rippability

Weaver, (1975) opined that geologist and engineers work hand in hand most times handling earth related issues. Their approach to the same problem is often widely different. Murphy III *et al.,* (2011) defines rippability as an effective property of a material and not in any way an intrinsic property. Rippability depends primarily on equipment being used and not observer invariant. This is basically a function of the strength of the ripping tool or machine as it strives to counter the resisting power of the rocks as entrenched in its density. It is possible to characterize unrippable crystalline rocks as being intact with low porosity, high ultrasonic and seismic velocity, high elastic modulus, high strength, high electrical resistivity, low fracture density and high rock quality designation (RQD) (Murphy III *et al.,* 2011).

Rippability is often classified in 3 categories qualitatively. It may be rippable, marginal and/or non rippable (Wickham, *et al.,* 1972; Jennings, *et al.,* 1970). It may be placed on a scale of 0-100 with 0 being highly rippable and 100 being unrippable. By and large, rippability is dimesnsionless (MacGregor, *et al.,* 1994).

2 Materials and methods

2.1 Data Acquisition

For this study, it was expedient to undertake the forward, reverse and intermediate shooting. The instruments adopted for this investigation include: cables, compass clinometers, D.C battery, geophones, GPS, hammer, plate, and seismograph. The instruments were then connected to the seismograph which record the signals picked up by the array of geophones after energy has been detonated through the weight drop using the hammer and plate. The battery serves as energy source to the seismograph itself. Twenty-four (24) channel full geophone array was used on a split spread pattern such that one of its ends is connected to the battery while the other end is connected to the hammer through the cable. Sequel to appropriate equipment set up, the seismograph was powered and armed, before shots were taken through the hammer against the plate to release energy. The records were adequately taken and saved on the seismograph for accessibility and in preparation for processing and interpretation. This was done severally to obtain a whole lot of data for different offsets namely 2m, 4m, 6m, 8/9,12/13 etc. Shots were taken for twenty-two (20) different profiles on a whole, with profiles P_{18}, P_{19} and P_{20} lying parallel to profiles P_{15}, P_{16} and P_{17}. Furthermore, all these six (6) profiles run perpendicular to profiles P_1-P_{14} (Figure 3). Elevation and bearing of location was observed using a GPS and compass enabled device.

2.2 Data Processing and Interpretation

Field data generated and stored were recalled from the seismograph, this was analyzed by picking the first arrivals using the 'SEISMIC IMAGER' computer software. The '*Pickwin'* module on the software assisted in plotting signals, signals were plotted with shot distances being plotted against arrival times as shown in Figure 2 using a geophone offset of 4m. A twenty-two (20) profile plot which consist of the forward, reverse, and intermediate were obtained. Then the first arrival times were picked before saving the first arrivals such that it can be later applied to obtain seismic refraction plots (see figures under results and discussion) using the *Plotrefrac*. Then the depth model was generated using the tomography as represented in Figures shown in results and interpretation section, such that velocity estimates were obtained to the top of the third (3rd) layer in order to have a near accurate seismic section. Invariably, the fourth (4th) layer (greater than 12m investigation) would not have been accurately described, hence not treated in details, since our zone of interest really lies above this layer. Numeric results obtained from all these are presented in table 6. From the seismic data, the velocities of sound were determined in the first, second, third and fourth layer.

3. Study area

The regional geology of the eastern Dahomey basin is as documented in (Burke *et al.,* 1971; Whiteman 1982; Omatsola and Adegoke, 1981; Slansky, 1962; Adegoke *et al.,* 1970; Ogbe, 1970; Kogbe, 1976; Rotimi *et al.,* 2014) this is as presented in Table 1. The study location has an area extent of approximately 1.2 Km^2 shown in Figure 3.

Table 1: Regional generalized stratigraphic setting of the eastern Dahomey basin SW, Nigeria.

AGE		FORMATION			LITHOLOGY
		Ako *et al.,* 1980	Omatsola and Adegoke, 1981		
TERTIARY	EOCENE	ILARO FORMATION	ILARO FORMATION		SANDSTONE
	PALEOCENE	OSHOSUN FORMATION/ AKINBO FORMATION	OSHOSUN FORMATION/ AKINBO FORMATION		SHALE
		EWEKORO FORMATION	EWEKORO FORMATION		LIMESTONE
CRETACEOUS	MASTRICHTIAN	ABEOKUTA FORMATION	ABEOKUTA GROUP	ARAROMI FORMATION	SHALE
	TURONIAN			AFOWO FORMATION	SANDSTONE AND SHALE
	BARREMIAN			ISE FORMATION	SANDSTONE
Undifferentiated Precambrian crystalline basement rocks					

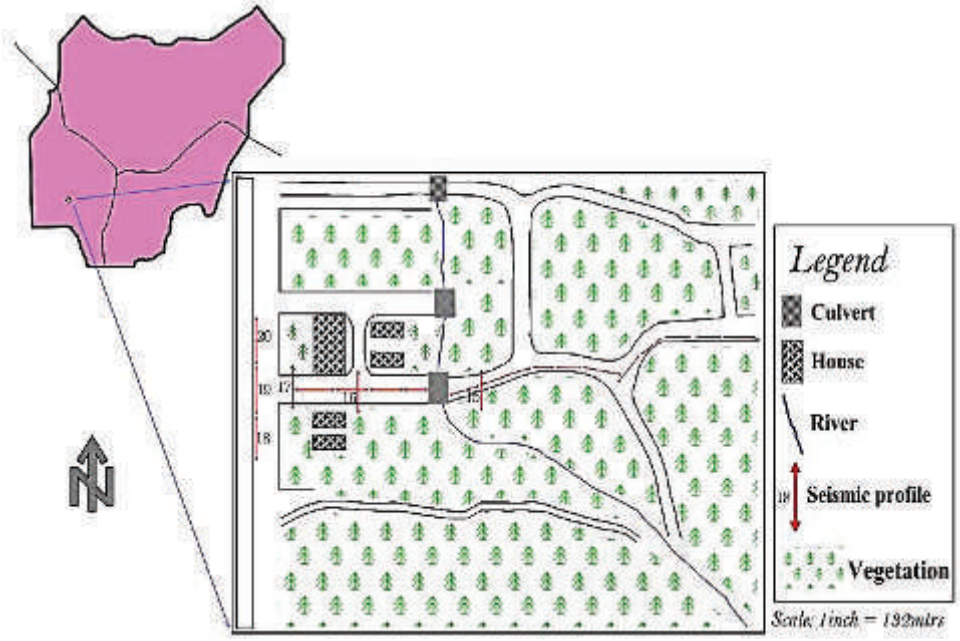

Figure 3: Location map of study area (Rotimi *et al.,* 2014)

4. Results and discussion

4.1 Layer 1

Recorded velocities for this layers across the 20 profiles traversed range from between 615 m/s – 930 m/s. The average value of 740 m/s and 4.4 m was recorded for velocity and layer thickness respectively. This layer from Rotimi et al., (2014), corresponded to the topsoil/regolith. This is grossly loose but stable. Ripping this unit will pose no resistance as it is just fairly consolidated (Figures 4-15).

4.2 Layer 2

The highest velocity recorded for this layer occurs across all profiles is approximately 1900m/s. the lithology modeled thickness is placed at between 3.27 m – 8.89 m. Average velocity for this layer is about 1535.21 m/s

and an average thickness of 5.32 m was realized. This units is interpreted as lateritic clay deposit upon which the topsoil/regolith of layer 1 is conformably laid. Ripping this unit will also be easy although it is evidently more compacted than layer 1. Being a lateritic clay deposit with fair compaction and sediment size less than 0.2 mm, lamination and fissility is hitherto immature and hence still a slightly compacted deposit (Figures 4-15).

4.3 Layer 3

This is the most compacted of the investigated subsurface unit. It can be inferred from the recorded velocities that it has higher density. The highest velocity of 2816.23 m/s was recorded across all 20 profiles. Layer thickness range from between 5.93 m to 12.22 m. this unit is interpreted as Sandy clay with patches of silt and alluvium. Porosity for this unit is expected to be good and permeability suspected to be fair. Good water bearing aquifer may be found in this layer which is supposed to boast of fair capillary pressure for fluid flow. Hence, source of ground water that can be explored for both domestic and industrial purposes. This unit is also rippable (Figures 4-15).

4.4 Layer 4

This layer is located well beyond 12 m and was sampled/ encountered beneath few of the 20 profile lines investigated. The velocity recorded here is greater than 2900 m/s and from literatures consist of lateritic sand, gravel and clay clastics generated from the underlying metamorphic basement protolith (Figures 5, 11, 13 and 15).

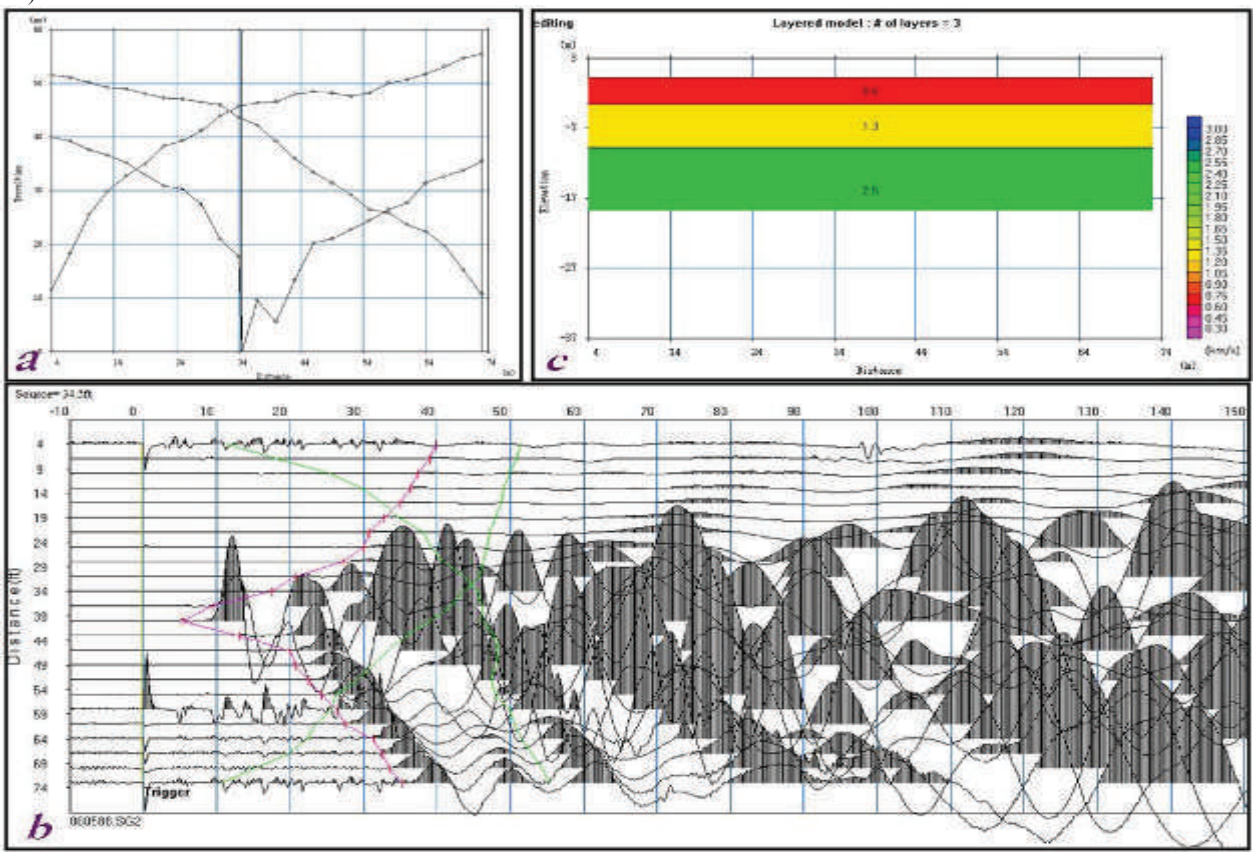

Figure 4.Various plot sections for Seismic refraction of Profile 3. (a) is Travel/ arrival time vs. distance chart, (b) Plot of arrival time vs. shot distance (c) Depth Model showing different layers obtained from seismic profile 3

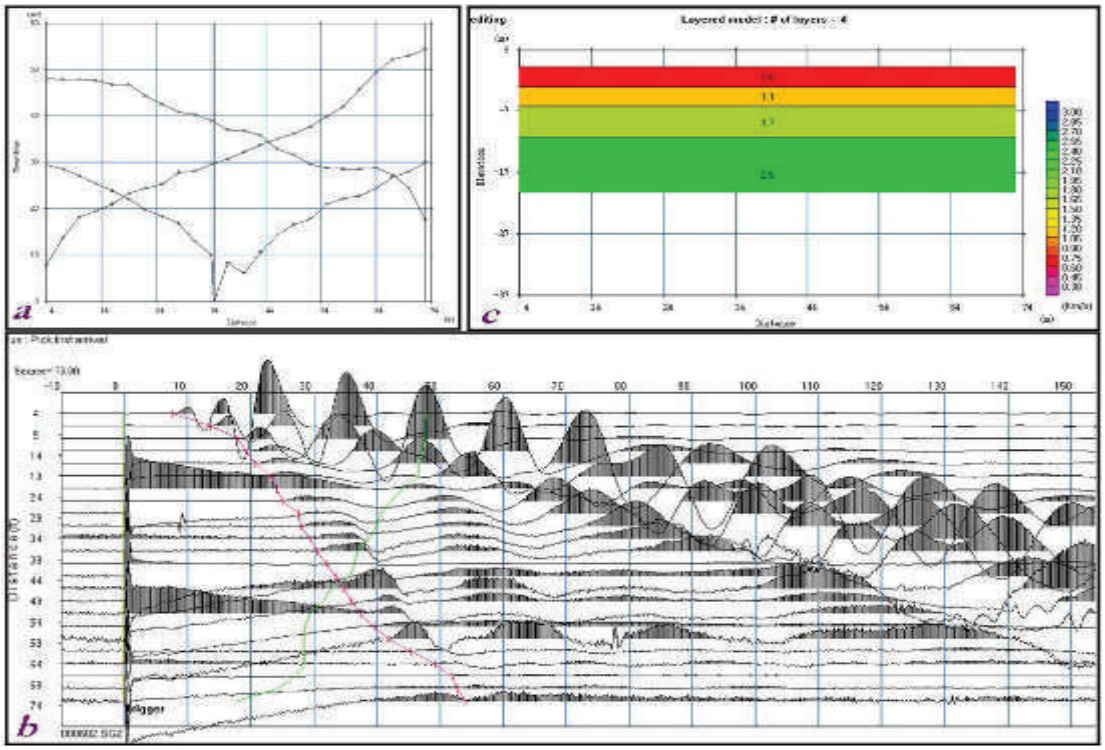

Figure 5.Various plot sections for Seismic refraction of Profile 4. (a) is Travel/ arrival time vs. distance chart, (b) Plot of arrival time vs. shot distance (c) Depth Model showing different layers obtained from seismic profile 4

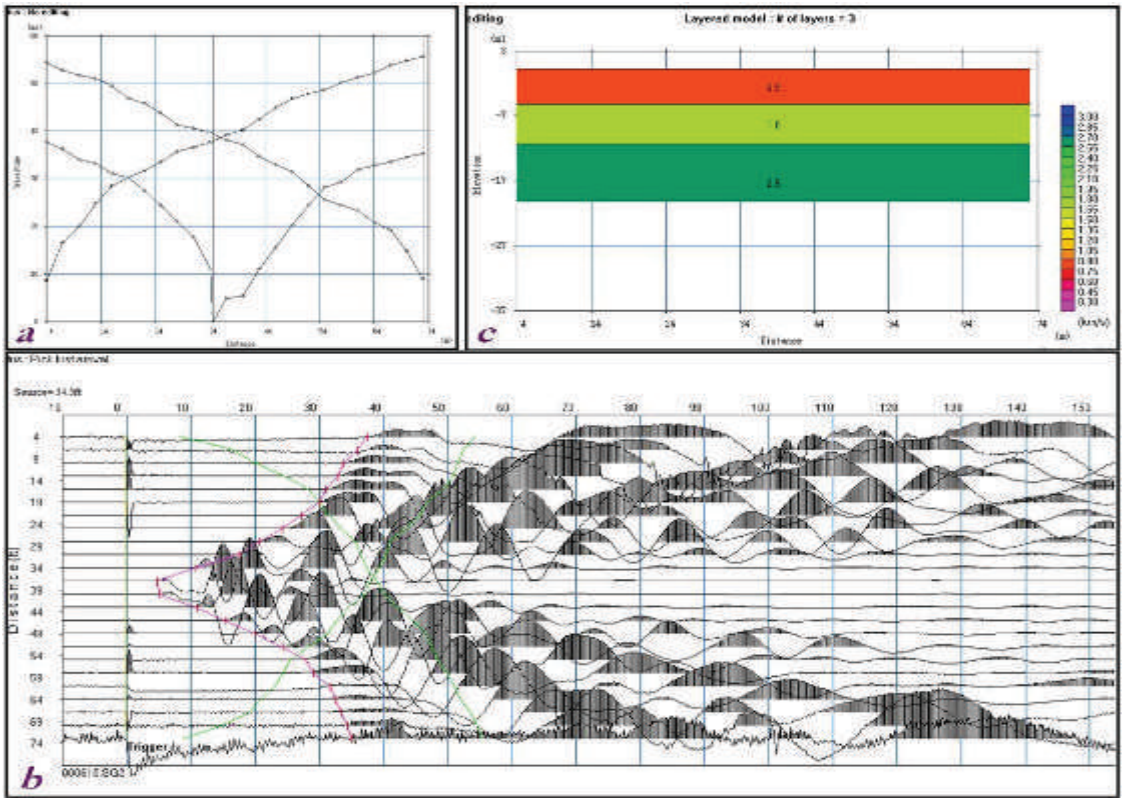

Figure 6.Various plot sections for Seismic refraction of Profile 5. (a) is Travel/ arrival time vs. distance chart, (b) Plot of arrival time vs. shot distance (c) Depth Model showing different layers obtained from seismic profile 5

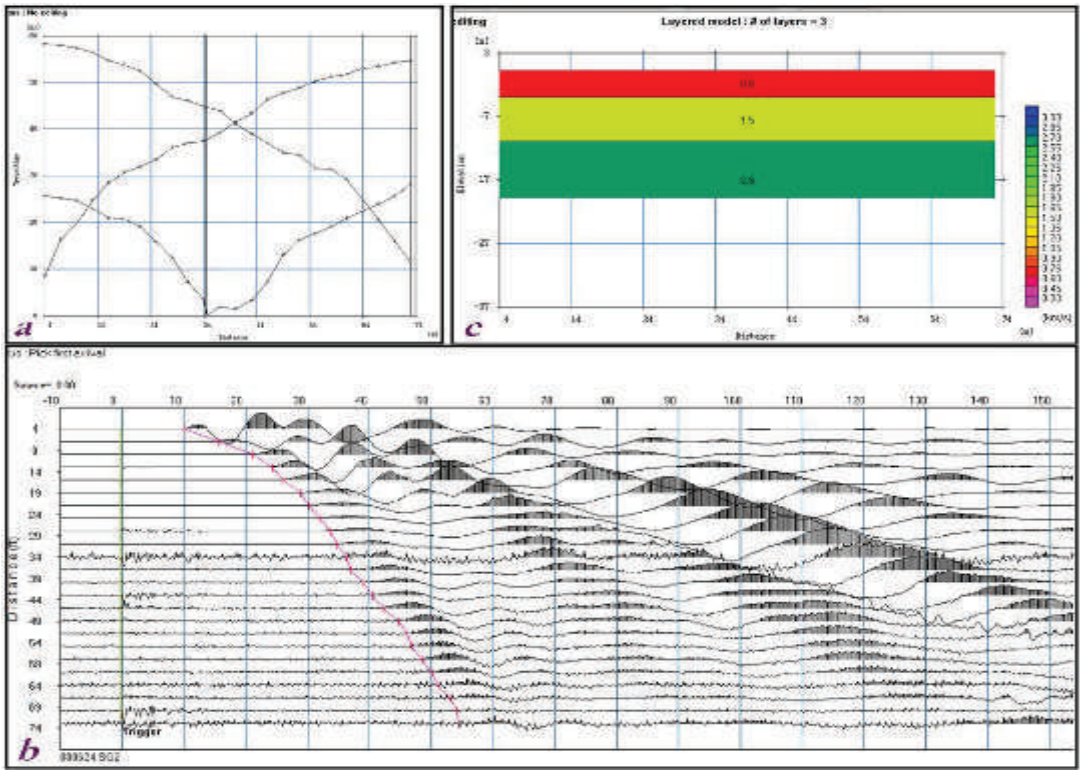

Figure 7.Various plot sections for Seismic refraction of Profile 6. (a) is Travel/ arrival time vs. distance chart, (b) Plot of arrival time vs. shot distance (c) Depth Model showing different layers obtained from seismic profile 6

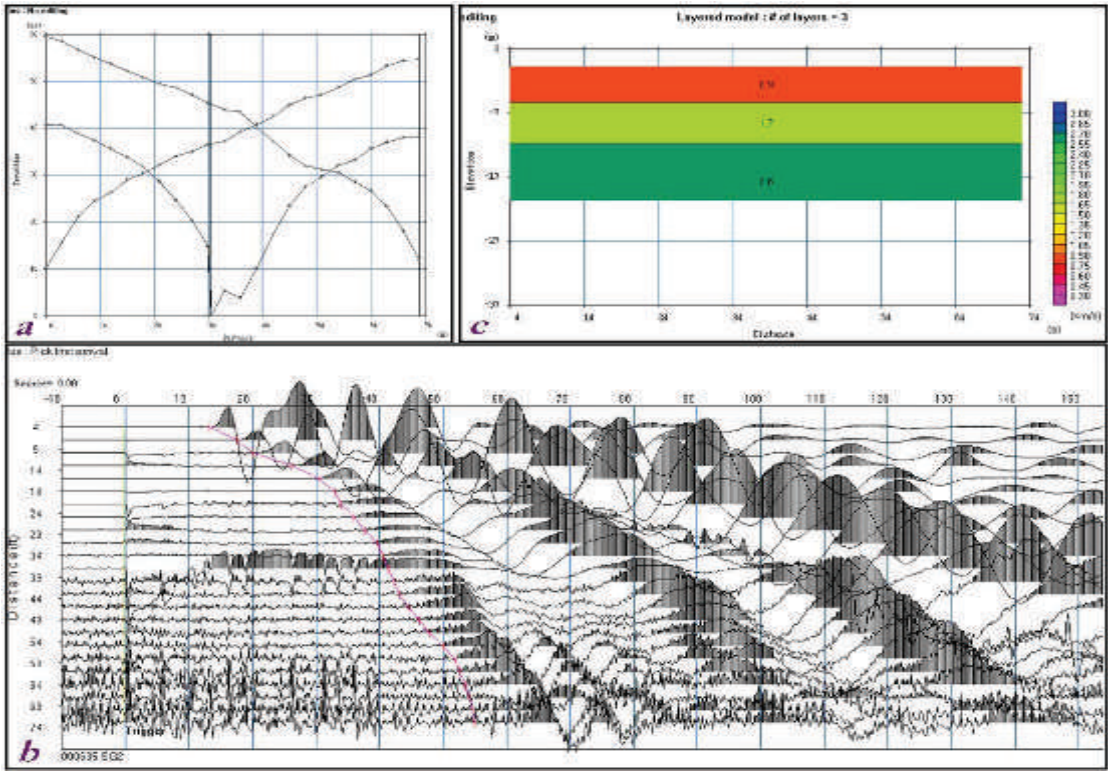

Figure 8.Various plot sections for Seismic refraction of Profile 7. (a) is Travel/ arrival time vs. distance chart, (b) Plot of arrival time vs. shot distance (c) Depth Model showing different layers obtained from seismic profile 7

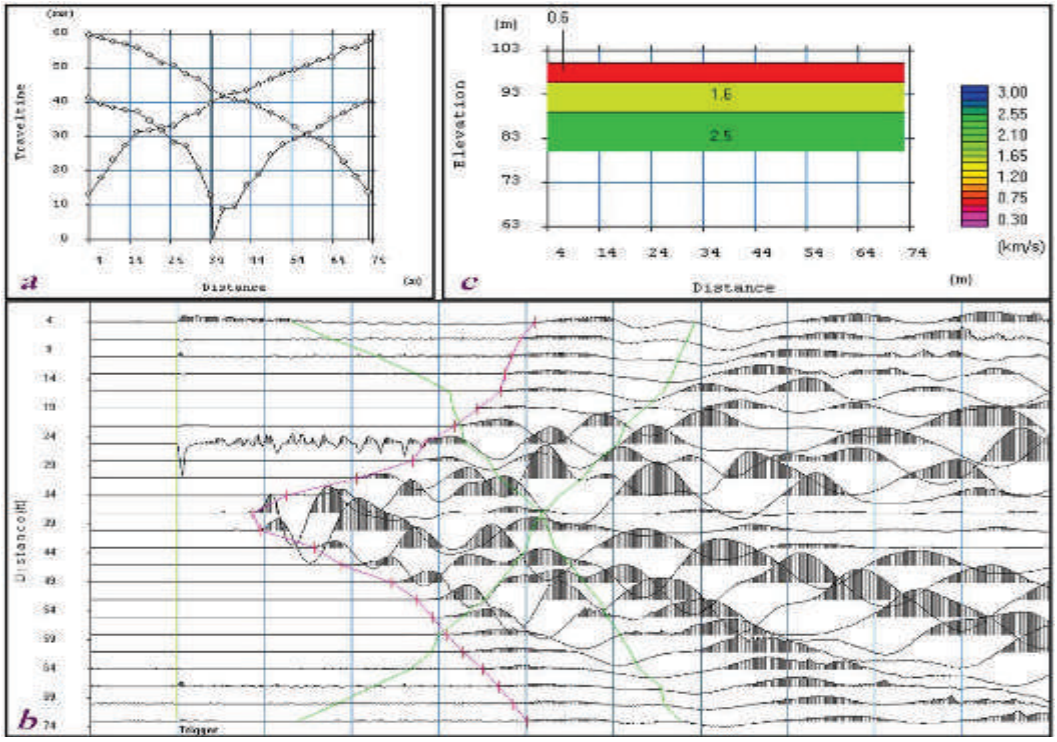

Figure 9.Various plot sections for Seismic refraction of Profile 8. (a) is Travel/ arrival time vs. distance chart, (b) Plot of arrival time vs. shot distance (c) Depth Model showing different layers obtained from seismic profile 8

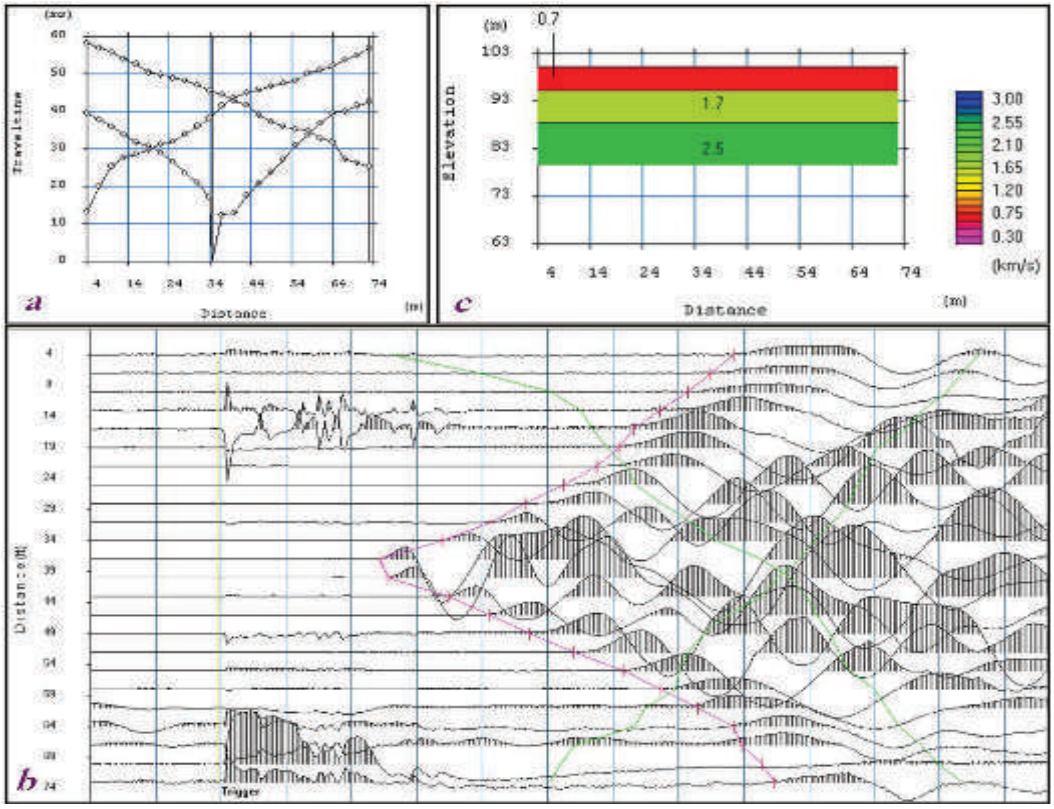

Figure 10.Various plot sections for Seismic refraction of Profile 9. (a) is Travel/ arrival time vs. distance chart, (b) Plot of arrival time vs. shot distance (c) Depth Model showing different layers obtained from seismic profile 9

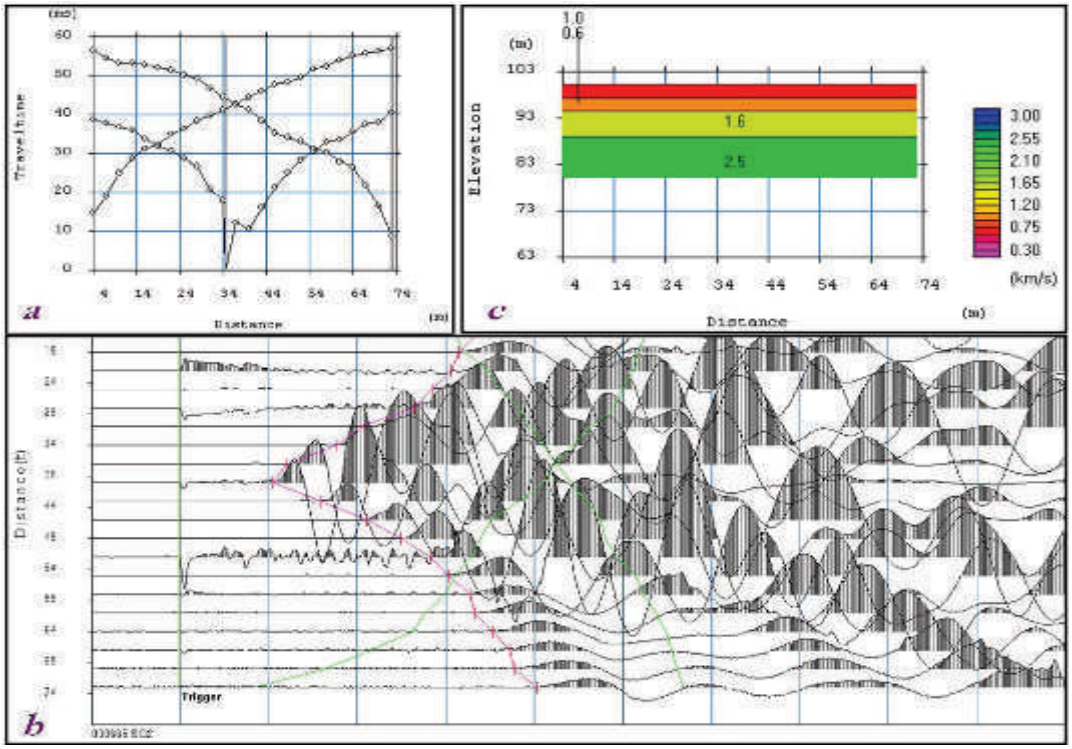

Figure 11.Various plot sections for Seismic refraction of Profile 10. (a) is Travel/ arrival time vs. distance chart, (b) Plot of arrival time vs. shot distance (c) Depth Model showing different layers obtained from seismic profile 10

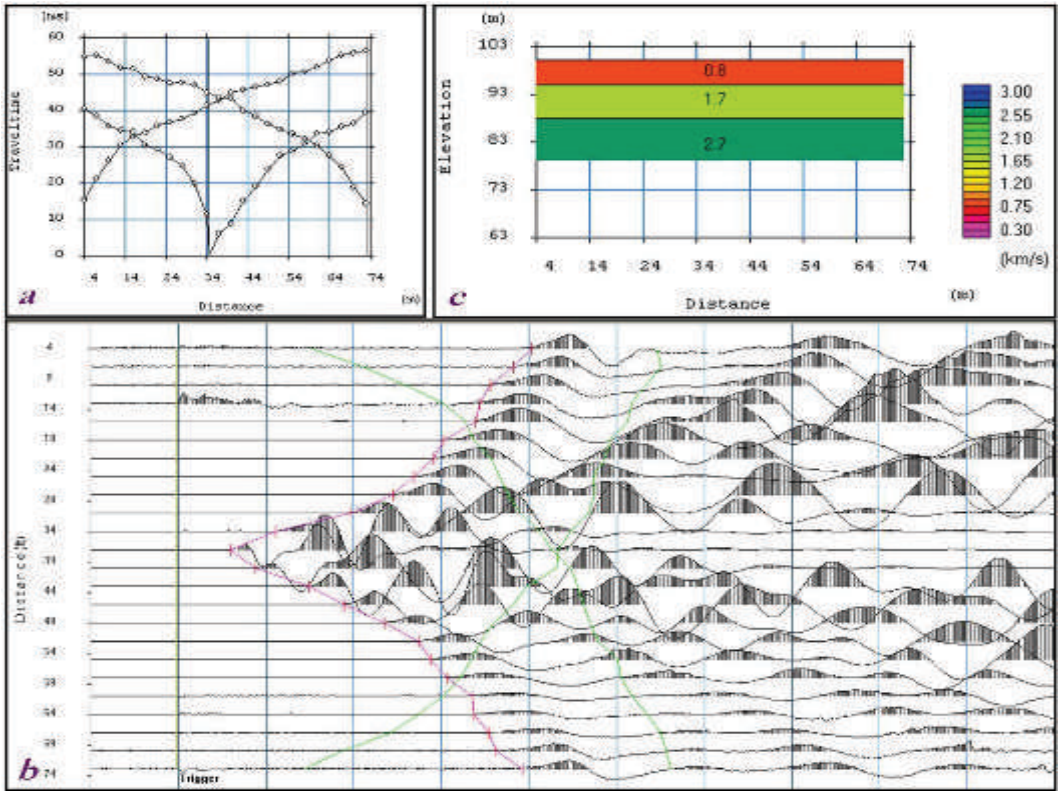

Figure 12.Various plot sections for Seismic refraction of Profile 11. (a) is Travel/ arrival time vs. distance chart, (b) Plot of arrival time vs. shot distance (c) Depth Model showing different layers obtained from seismic profile 11

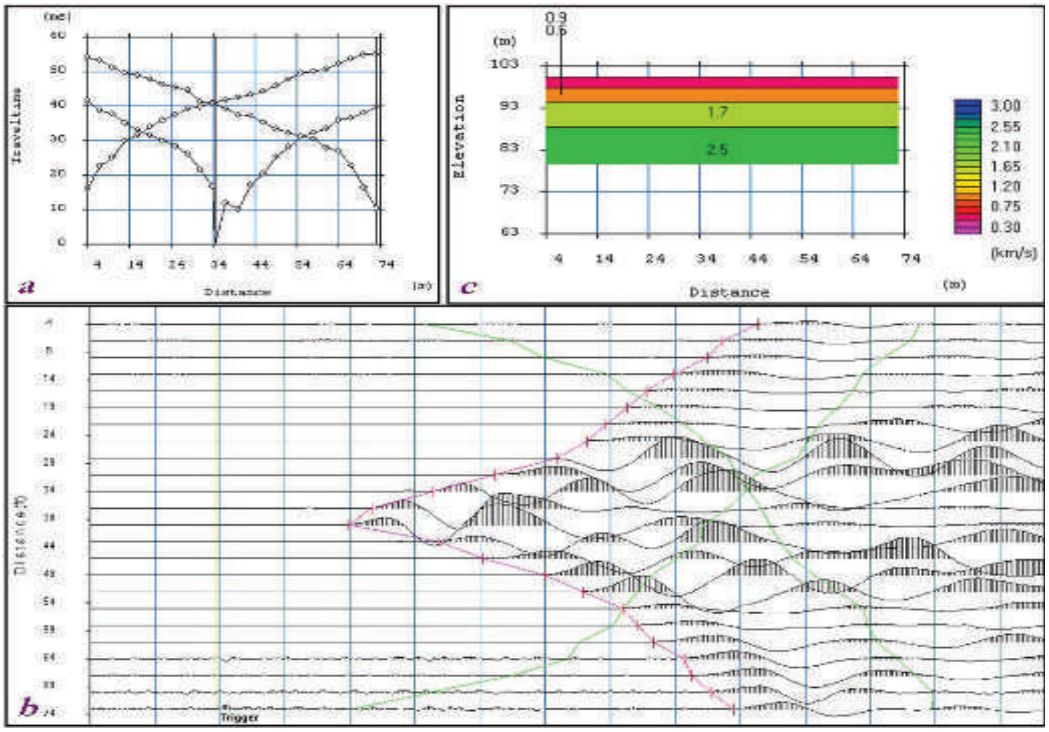

Figure 13.Various plot sections for Seismic refraction of Profile 16. (a) is Travel/ arrival time vs. distance chart, (b) Plot of arrival time vs. shot distance (c) Depth Model showing different layers obtained from seismic profile 16

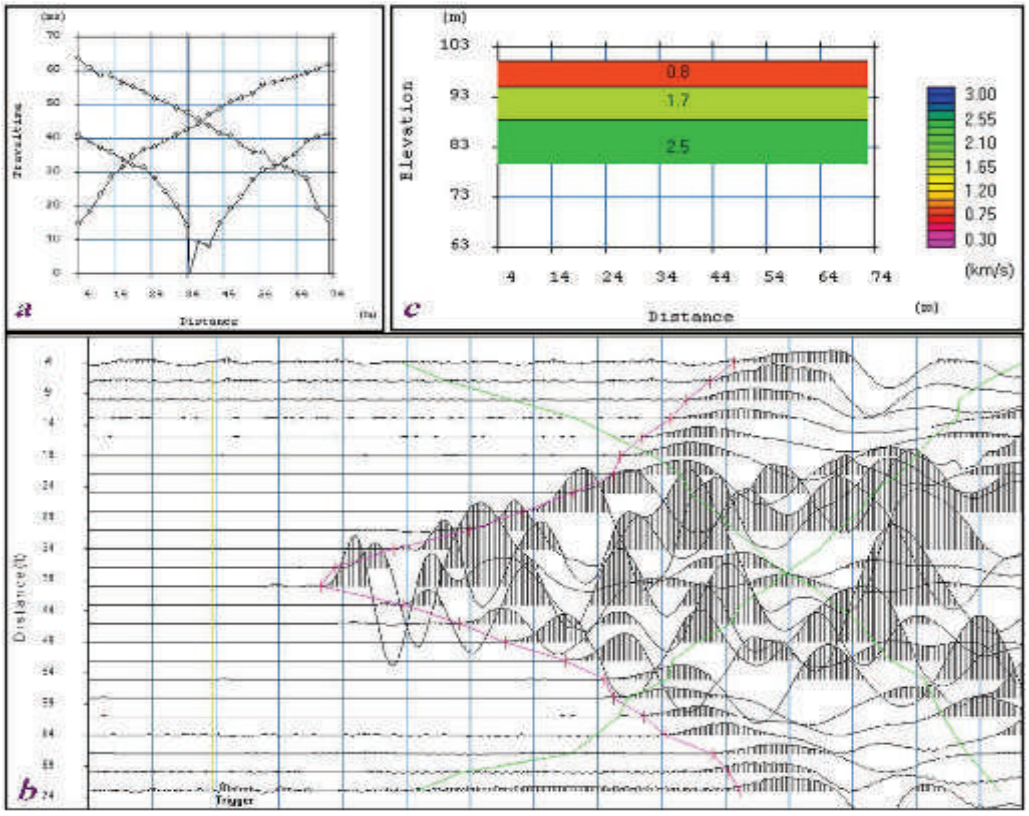

Figure 14.Various plot sections for Seismic refraction of Profile 17. (a) is Travel/ arrival time vs. distance chart, (b) Plot of arrival time vs. shot distance (c) Depth Model showing different layers obtained from seismic profile 17

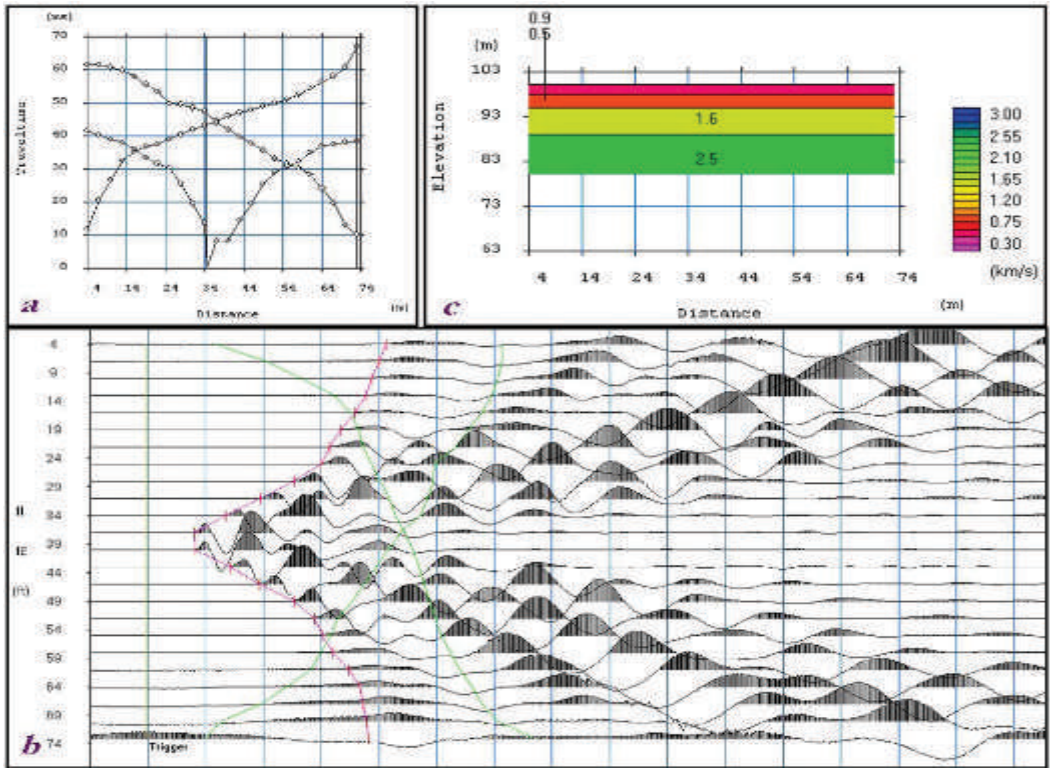

Figure 15.Various plot sections for Seismic refraction of Profile 20. (a) is Travel/ arrival time vs. distance chart, (b) Plot of arrival time vs. shot distance (c) Depth Model showing different layers obtained from seismic profile 20

5. Conclusion

The rippability potential of the Sedimentary rocks of in Jubilee Parkland Estate, Southwestern Nigeria has been analyzed and the following conclusions can be drawn;

1. The respective profiles (20) on the location have been surveyed with subsurface layers delineated, where some have 3 layers and others 4 layers. There is an increase in seismic velocity with depth which obeys the natural concept, and average velocities of each layer have been obtained. First layer is 740 m/s, second layer is 1,535.21 m/s, third layer is 2,310 m/s and fourth layer - 2,900 m/s, all average values.
2. Vertical thickness of this location is in excess of 12 m and the respective lithologies are highly weathered with an easily achievable rippability range of easy to hard.
3. The thickness of each layer has also been presented with layer 1 (4.4m) composed mainly if regolith, layer 2 (5.32 m) made up of lateritic clay deposit, layer 3 (5.93-12.22 m) consisting of sand, clay and patches of silt and alluvium; and layer 4 (>12m) composed of clay, clastics, lateritic sand and gravel. Probable ground water source has been identified as layer 3 which can be exploited for both industrial and domestic use.

Acknowledgement

The author appreciates the support of MOST-CASTEP for equipment and workstation provided. The inputs of field assistants are also recognized for making data acquisition processes smooth and fruitful

References

Adegoke, S.O., T.F.J. Dessauvagie and A.J. Whiteman, (1970); Macrofauna of Ewekoro Formation (Paleocene) of S.W. Nigeria, (In) African Geology. Univ. of Ibadan, pp: 269-276.
Bailey, A.D., (1975); Rock types and seismic velocity versus rippability, *in* Proceedings of the 26th Annual Highway Geology Symposium, Coeur d'Alene, Idaho, August 13–15, 1975, p. 135–142.
Bieniawski, Z.T., (1973); Engineering classification of jointed rock masses. Trans SA Instn of Civ Engrs, Vol 1 5, No 12, pp335 - 344.
Burke, K.C.B., T.F.J. Dessauvagie and A.J. Whiteman (1971); Opening of the gulf of guinea and geological history of the Benue Depression and Niger Delta. Nat. Phys. Sci., 233: 51-55
Caterpillar Performance Handbook (2010); Edition 36, Caterpilar, Peoria, II.
Church, H.K., (1974); Two exceptions to seismic principles. World Construction, Vol 27, No 5, pp26 - 32.
Earthworks, (2003); "Surface geophysical exploration: Newark Bay and Arthur Kill Channels, Arthur Kill rock

evaluation". USACE-NYD, USACE-NYD DACW51-02-D-005, IDC 180, Delivery Order 0003
Jennings, J.E., and Robertson, A. Macg., (1970); The stability of slopes cut into natural rock. Proc Int Symp on Soil Mechanics. Pp585 - 590.
Kearey, P. and Brooks, M., Hill I., (2002); An introduction to geophysical exploration. Blackwell Scientific Publication, Oxford, pp 198-217.
Kogbe C.A., (1976); The Cretaceous and Paleogene sediments of southern Nigeria. In C. A. Kogbe (Ed.) Geology of Nigeria. Pp. 325-334.
MacGregor, F., Fell, R., Mostyn, G.R., Hocking, G., and McNally, G., (1994); The estimation of rock rippability: Quarterly Journal of Engineering Geology, v. 27, p. 123–144.
Murphy III, W.F., Ward, W.B., Boyd, B., Murphy IV, W.F., Nolen-Hoeksema, R., Art, M Rosales-R, D.A. (2011); "Geophysical, geological, geotechnical and mechanical testing of rock," Proceeding of the Western Dredging Association (WEDA XXXI) Technical Conference and Texas A&M University (TAMU 42) Dredging Seminar, Nashville, Tennessee
Ogbe, F.A.G., (1970); Stratigraphy of strata exposed in Ewekoro quarry western Nigeria (In) Africa geology (T.F.J. Dessauvage and A.J. Whiteman, Eds.), University of Ibadan, Pp: 305-324.
Omatsola M. E., Adegoke O.S., (1981); Tectonic Evolution of Cretaceous stratigraphy of the Dahomey Basin. J. Min. Geol. 18(1), 130-137.
Reynolds, J.M., (1997); An introduction to applied and environmental geophysics: Wiley, 796 p.
Rotimi O. J., Atunbi J. F., and Oshunnuga B., (2014); Groundwater prospecting using Electrical Resistivity profiles over Jubilee Homes Parkland, Southwest, Nigeria. Journal of Emerging Trends in Engineering and Applied Sciences (JETEAS) 5(3): 188-196
Sharma, P.V., (1997); Environmental and engineering geophysics: Cambridge, United Kingdom, Cambridge University Press, 475 p.
Slansky M., (1962); Contributional etude Geological du Basin sedimentative corfell all Dahomey at du too Bearaeu du Kuchercher Geologue at Mounever memoir, pp. 11-12.
Smith J. Hardy, (1986); Estimating Rippability by Rock Mass Classification. Engineering Geology and Rock Mechanics Division, Geotechnical Laboratory. The 27th U.S. Symposium on Rock Mechanics (USRMS), 23-25 June, Tuscaloosa, Alabama. 1986. American Rock Mechanics Association
Weaver J. M., (1975); Geological factors significant in the assessment of rippability. Die Siviele Ingenieur in Suid Afrika. Reproduced by Sabinet gateway under license from producer. Pp. 313 - 316
Whiteman A., (1982); Nigeria: Its Petroleum Geology resources and potential, Graham and Trotman Ltd. 1: 166.
Wickham, G.E., Tiedemann, H.R., and Skinner, E.H., (1972); Support determinations based on geologic predictions. Proc 1st American rapid excavation and tunneling conf. AIM E. Pp43 - 64.

The IISTE is a pioneer in the Open-Access hosting service and academic event management. The aim of the firm is Accelerating Global Knowledge Sharing.

More information about the firm can be found on the homepage:
http://www.iiste.org

CALL FOR JOURNAL PAPERS

There are more than 30 peer-reviewed academic journals hosted under the hosting platform.

Prospective authors of journals can find the submission instruction on the following page: http://www.iiste.org/journals/ All the journals articles are available online to the readers all over the world without financial, legal, or technical barriers other than those inseparable from gaining access to the internet itself. Paper version of the journals is also available upon request of readers and authors.

MORE RESOURCES

Book publication information: http://www.iiste.org/book/

Academic conference: http://www.iiste.org/conference/upcoming-conferences-call-for-paper/

IISTE Knowledge Sharing Partners

EBSCO, Index Copernicus, Ulrich's Periodicals Directory, JournalTOCS, PKP Open Archives Harvester, Bielefeld Academic Search Engine, Elektronische Zeitschriftenbibliothek EZB, Open J-Gate, OCLC WorldCat, Universe Digtial Library , NewJour, Google Scholar